PARTICLE MOTION IN A STANDING WAVE LINEAR ACCELERATOR*

E.E. Chambers
High Energy Physics Laboratory, Stanford University
Stanford, California

I. CASE I: ON AXIS

1. Traveling Wave Review

The traveling wave electron accelerator is not simpler than the standing wave machine, but it is better understood. So, with the object of understanding, let us look at the first section of a traveling wave accelerator where the wave velocity β is less than 1.

According to the equations derived in the Appendix, after Slater,[1] the momentum-phase diagram is shown in Fig. 1a. The phase angle, φ, is here defined as the angle by which the electron leads the crest of the traveling wave, and P is the momentum of the electron. Apparently, Slater chose to call phase zero when the particle is $\pi/2$ ahead of the wave crest because there is symmetry about the line $\varphi = \pi/2$ with a traveling wave.

In accordance with Eq. (8) of the Appendix, a function

$$f(\varphi) \equiv H + \frac{\alpha}{2\pi} \sin \varphi = E(P) - \beta P \equiv f(P) \quad , \tag{1}$$

can be defined where H is the Hamiltonian, α is the field intensity, and E and P are the energy and momentum of the electron, all in dimensionless units.

Figure 1b shows the relationship between φ and P through the function f. The shape of the curve depends only on the wave velocity β. The minimum value of f(P) allowed by

$$f(P) = E(P) - \beta P$$
$$\frac{df}{dP} = v - \beta = 0 \quad , \tag{1a}$$

where $\dot{v}$ is the reduced particle velocity, is $f_1(P_1) = 1/E_1$, where $E_1 = (1 - \beta^2)^{-\frac{1}{2}}$ and $P_1 = \beta E_1$ are the energy and momentum of a particle moving at the traveling wave velocity.

The maximum and minimum values of f(φ), being f_2 and f_3 respectively, allowed by

$$f(\varphi) = H + \frac{\alpha}{2\pi} \sin \varphi \quad , \tag{1b}$$

are $f_2 = H + \alpha/2\pi$, and $f_3 = H - \alpha/2\pi$, where H is determined by the initial condition through

---

1. J.C. Slater, Rev. Mod. Phys. 20, 473 (1948).

$$H = E - \beta P - \frac{\alpha}{2\pi} \sin \varphi \quad . \tag{1c}$$

If H is less than its critical value, $H_c = 1/E_1 + \alpha/2\pi$, $f_3 < f_1$, and the orbit of the particle is like orbit 1 of Figs. 1a and 1b. If $H > H_c$, $f_3 > f_1$, and the orbit is like either orbit 2 or 3 of Fig. 1a, depending on the initial conditions.

Figures 2 through 5 show graphs plotted by computer. They are segments of the closed orbits of Fig. 1a. The lines labeled 0 - 0, 1 - 1, etc. show the locus in phase space of electrons at a given distance along the accelerator. The momentum scale was chosen to show desired features best; a constant times $\log(1 + 2P/mc)$ is plotted. In Fig. 2, fourteen electrons start out along line 0 - 0 at 80 keV. The four starting with $\varphi \geq 140^{\circ}$ were approaching $P = 0$, and it was not considered fruitful to follow them further. The line 1 - 1 shows where the remaining ten electrons were after passing through $1/16 \, \lambda$. Between the two smallest orbits are contained all the electrons injected between 70° and 110°. If extracted at $v = \beta$, they would span 7° in phase; if extracted at the end of a wavelength (on line 4 - 4), they would span 8°. It is also interesting that the electrons injected between 60° and 90° could be extracted in a 2° bunch at the end of $1 \, \lambda$. Figure 3 is for half the accelerating field, Fig. 4 for a more rapidly traveling wave, $\beta = 0.9$, and Fig. 5 for $\beta = 1.0$ ($P_1 = \infty$).

2. Standing Wave at Low Energy[*]

At low energies, the trajectories in $P - \varphi$ space of particles which are captured in standing wave linacs (1) cross and recross, (2) have kinks every half wavelength, (3) decrease in momentum at first, and (4) slip about twice as much in phase as one would expect from the corresponding traveling wave case.

Figure 6 shows the orbits in $P - \varphi$ space for particles accelerated by a standing wave. The graphs do not close on themselves; they do cross. There is hardly a perceptible kink in the curves at the end of $1 \, \lambda$ ("2" on the graph) because it just happens that v very nearly equals β at this point so that the curves are vertical.

Figure 7 gives a very much enlarged view, for 2.5 wavelengths of standing wave accelerator, of a very small segment of a locus such as 4 - 4 in Fig. 4. The locus is the ends of orbits such as those at "10" in Fig. 6. An input of $\Delta\varphi$ of 20° has been bunched to 1° ($1 - \cos 0.5^{\circ} = 0.4 \times 10^{-4}$) with an energy spread of 0.064 mc^2 (1.5% of present energy, but 0.3×10^{-4} of 1 GeV). A 9° initial $\Delta\varphi$ ($69.5^{\circ} - 78.5^{\circ}$) would give 0.15% of present energy. The curve for 79.9 kV shows that the φ_0 of the "bunch" is fairly independent of γ_0, but the point "B" is where "A" would move for 79.0 kV and indicates that a variation of the 80 kV by 1.2% would affect the resolution to the extent that the phase spread contribution to the energy spread would be $\sim 10^4$.

In order to establish at least the direction of the gradient of good energy resolution in the multidimensional space of buncher design (α, β_1, β_2, ... length), a large number of calculations were made. Some results for a half wavelength of standing wave accelerator are presented in Fig. 8 whose straight lines attest to the roughness of approximations made in constructing the figure. The trends, however, are not approximate: (1) good bunches are fairly independent of β; (2) low field strengths give better bunches. Two quantitative conclusions were drawn: (1) since a $\Delta E/E$ of 1×10^{-4} is the goal, $\alpha < 2$ would unnecessarily sacrifice fast acceleration where it is most desirable (to arrest transverse velocity); and (2), $\beta = 1$ eliminates problems that might arise

---

from other choices. (For instance, $\beta = 1$ makes the accelerating field of the fundamental frequency independent of the distance off axis.)

The calculations leading to Fig. 9 were made in order to design a combination buncher and injector section for a superconducting linac. Notwithstanding the possible advantages of $\beta = 1$, the real advantage of increasing the kinetic energy (for $Z = 2.5 \lambda$, from 1.6 to 2.6 MeV) by going to $\beta = 0.95$ was considered worthwhile. The approximate length was determined by how much was needed to become relativistic.

Figures 10 and 11 indicate how the bunch is formed. Continuously injected electrons would be represented at the moment of injection ($Z = 0$) by the line with unit slope. The dotted lines on Fig. 10 show where the electrons are in the first half wavelength when the fundamental rf electric field changes sign. Electrons with $160°$ $< \varphi_0 < 180°$ are stopped at $Z \gtrsim \lambda/8$. Electrons with $-180° < \varphi_0 < 100°$ stop before $\lambda/4$ even though they were initially accelerated. Electrons injected at $-100°$ ($180°$ from bunch) would be stopped at $Z \approx \lambda/4$ and $\varphi \approx 180°$ and presumably would be rejected with 80 kV back at the gun. With continuous injection, 5% ($\Delta\varphi_0 = 20°$) will come out in a tight bunch, 25% will come out badly spread in phase and energy, 35% will stop before $\lambda/4$, many of which may be "rejected," but the other 35% get beyond $\lambda/4$ and it is most likely that they will end up as heat in the cavity wall. Figure 11 for $\beta = 0.95$ shows the bunch gaining on the wave between $Z = \lambda$ and 2.5λ. It is by proper choice of α, β and length that the bunch ends with $\varphi \to 0$ for maximum energy gain; it is not necessary for good bunching.

There appears to be an understandable characteristic of the bunch. It passes where ($\lambda/4$) the field is maximum when ($\varphi = 0$) it is maximum.

3. Standing Wave at High Energy

After the energy of an electron is a few MeV, the effect of the backward traveling wave component on the <u>longitudinal</u> coordinates of an electron is completely negligible in a standing wave accelerator.

II. CASE II: OFF AXIS

1. Introduction

In a superconducting accelerator where high energy resolution is possible, the radial motion is particularly important because of its effect on monitoring and controlling the energy of the beam.

Figure 12 is an attempt to show the whole problem at a glance. Radial momentum is plotted against distance off axis. The circle represents a set of particles as they are injected into a short section of accelerator. The dots trace the path in this phase space of a particle started at unit distance off axis. The set of particles at the middle of the first cavity is represented by the fat ellipse, but the dots show that large excursions of momentum have occurred. At the end of the first cavity the set is represented by the long thin ellipse. If the dots were continued they would fill in most of the space between the dots shown. At the end of five cavities, the set is represented by the remaining ellipse. Note that the ellipses represent a set of particles at certain stages of acceleration: the dots represent the orbit of one particle.

Figure 12 represents radial motion in the first accelerator section. It is complicated and will be treated last.

First, the case will be treated in which the particle has its energy much greater

than its rest mass and much greater than the energy gained per wavelength. Next the restriction on the energy gradient will be dropped, and last, an injection section will be considered.

Definitions of symbols are given in the Appendix.

2. Very High Energy, Relativistic Particles

The equation of radial motion is

$$\frac{d}{dz}\left(\gamma\frac{dr}{dz}\right) = -2\pi\,\alpha r\,\sin 4\pi z \ , \tag{2}$$

which is linear in r, r', and r'' so that all solutions may be scaled. The equation of axial motion integrates to

$$\gamma = \alpha\left(z - \frac{\sin 4\pi z}{4\pi}\right) \ , \tag{3}$$

where a small liberty has been taken with the constants of integration by requiring that $z_0 = \gamma_0/\alpha$ and z_0 is integer or half integer.

The sine in each of Eqs. (2) and (3) is the result of the backward traveling component of the standing wave. The contribution to the radial force from E and v X B identically cancel in the forward traveling component.

Combining Eqs. (2) and (3) and the definition of radial momentum, and letting $x = 4\pi z$

$$\frac{dP}{dx} = -\frac{r}{2}\sin x \quad , \tag{4a}$$

$$\frac{dr}{dx} = \frac{P}{x - \sin x} \quad . \tag{4b}$$

Equating both the sines in Eq. (4) to zero, the traveling wave solution is found to be

$$P = P_0 \quad , \tag{5a}$$

$$r = P_0\ln\frac{x}{x_0} + r_0 \quad . \tag{5b}$$

Using this r as a first trial solution, and integrating by parts to increase the power of $x - x_0/x$, a solution correct to the first order in $(x - x_0)/x$ was found:

$$P = P_0\left[1 + \frac{\cos x}{2}\ln\frac{x}{x_0} - \frac{\sin x}{2x}\right] + r_0\left[-\frac{2\cos x + 1}{8}\ln\frac{x}{x_0}\right.$$

$$\left. + \frac{\cos x - 1}{2} + \frac{\sin x}{4x}\left(1 - \frac{\cos x}{2x}\right)\right] \tag{6a}$$

$$r = P_0\left[\ln\frac{x}{x_0}\right] + r_0\left[1 - \frac{1}{2}\ln\frac{x}{x_0} + \frac{\sin x}{2x}\right] \quad . \tag{6b}$$

None of the terms in Eq. (6) is a result of the sine in Eq. (4b); that is, the intra-cavity change in mass is not a first order effect.

As indicated in Fig. 12, the gyrations within a cavity may be large compared with the net change across a cavity which is of chief importance. Letting $x - x_0 = 2\pi$, and $x_0 = 2\pi n$, the effect of the $(n + 1)^{th}$ cavity is given by the difference equations:

$$P(n + 1) - P(n) = \frac{1}{2n} P(n) - \frac{3}{8n} r(n) \quad , \tag{7a}$$

$$r(n + 1) - r(n) = \frac{1}{n} P(n) - \frac{1}{2n} r(n) \quad , \tag{7b}$$

which again are good to first order in n^{-1}.

A solution which satisfies Eq. (7) to first order in n^{-1} is

$$P(n) = \sqrt{3}\, P_0 \sin (L + \theta) - 3(8)^{-\frac{1}{2}} r_0 \sin L \quad , \tag{8a}$$

$$r(n) = 2\sqrt{2}\, P_0 \sin L + \sqrt{3}\, r_0 \sin (\theta - L) \quad , \tag{8b}$$

where $L = (8)^{-\frac{1}{2}} \ln n/n_0$ and $\sin \theta = (3)^{-\frac{1}{2}}$.

Equation (8) is plotted in Figs. 13 and 14. The solid triangles on each curve indicate the points up to which the curves were checked against a very accurate computer calculation that started with $Z_0 = 100 \lambda$. The n's of Eq. (8) can be interpreted as energy. The particle will cross the axis after it has increased its energy to 5.7 times its initial energy if its initial radial momentum is zero. From the time the particle crosses the axis, its radial momentum will continue to increase until its energy is increased by a factor of 15 and its radial displacement will increase until its energy is increased by a factor of 85; it will recross the axis again at energy factor $(85)^2$.

From the equations, it appears that the maximum radial excursion will be minimized if $P_0 = \frac{1}{2} r_0$, and further that a complete cycle of radial motion will be made every time the energy is increased by a factor of 5×10^7.

Comparing the standing and traveling wave radial motion over an energy increase of a factor of e,

Standing Wave	Traveling Wave
$P = \frac{3}{2} P_0 - \frac{3}{8} r_0$	$P = P_0$
$r = P_0 + \frac{1}{2} r_0$	$r = P_0 + r_0$

it appears that there is a significant difference from the Lorentz contracted drift tube analogous to the traveling wave accelerator.

As suggested by the eigenvector found during the solution of Eq. (7), let $Q = 2\sqrt{2/3}\, P$,

$$Q = Q_0 \cos L + (\sqrt{2}\, Q_0 - \sqrt{3}\, r_0) \sin L \quad , \tag{9a}$$

$$r = (\sqrt{3}\, Q_0 - \sqrt{2}\, r_0) \sin L + r_0 \cos L \quad . \tag{9b}$$

The maximum values of Q and r are each equal to K which is a constant of the motion and $K^2 = 3Q^2 - 2\sqrt{6}\, Qr + 3r^2$. If the axes are rotated 45° and K is magnified to unity,

$$x = \frac{Q + r}{\sqrt{2}\, K} \quad \text{and} \quad y = \frac{Q - r}{\sqrt{2}\, K} \quad .$$

$$x = x_o \cos L + (\sqrt{3} + \sqrt{2}) \, y_o \sin L \quad , \tag{10a}$$

$$y = - (\sqrt{3} - \sqrt{2}) \, x_o \sin L + y_o \cos L \quad . \tag{10b}$$

From this, the constant of the motion is found to be

$$\frac{x^2}{1 + \sqrt{2/3}} + \frac{y^2}{1 - \sqrt{2/3}} = 1 \quad . \tag{11}$$

The ellipse found in Eq. (11) is shown in Qr space in Fig. 15; its area is $\pi K^2 / \sqrt{3}$. This ellipse is a trajectory as contrasted with the ellipses of Fig. 12 which represented sets of particles.

3. Relativistic Particles

If γ_0 is not much greater than α, the analysis of the previous section does not apply, but this can only be the case over only a few wavelengths because $\gamma = \alpha z$ for relativistic particles.

To investigate this, computer calculations were made over one-half wavelength and the results plotted in Fig. 16. In a drift tube, the particle represented by the dot on the circle would have moved directly to the dot at its right. If $z_o = 10 \, \lambda$, the difference is slight. If $z_o = \lambda$, the difference is significant.

The simple conclusion is that for $z > 10$ the analysis of the previous section is adequate, for $z > 100$ it is as good as the computer, and for $z < 10$ the computer should be used.

4. The Injector Section

Consideration of the injector section is not complete, but some calculations have been made. The tentative conclusion is that, in first order, even this section acts like a drift tube if the gyrations within a cavity are not considered. Figure 17 shows the effect of acceleration from 80 keV to 100 MeV. In the injector section, i.e. during the first 2λ, besides the drift tube effect of tilting the ellipse forward there is a slight defocusing in that the absolute values of all momenta are increased by about 30%. In the next 10 λ, after the axial phase is set to zero, the particles (two of which are represented by dots on the curve) move much as would be expected from the analysis of the high energy section. The next two sections of 20 λ each continue to accelerate as expected. If a 20° axial phase bunch had been injected, the set (in radial phase space) that was first to be injected (10° early) and the set last to be injected are shown separately at 52 λ. Clearly, the radial phase space problem in a standing wave injector is soluble.

Figure 18 shows the results of some calculations on another injector section. To get a feeling for the problem the question was asked, "What is necessary to get a parallel beam out of the injector?" Electrons were put in $\lambda/60$ off axis and the answer depends strongly on axial phase. For an electron in the middle of the axial bunch, the answer is that it should be aimed at a point on the axis $f = 1.8 \, \lambda$ into the accelerator. For those with different axial phase, the answer is different, as shown in the table:

$\varphi - \varphi_o$	f/λ
10°	0.75
5°	1.0
0	1.8
-5°	2.7
-10°	∞

For a given r_o in the high energy section, the radial phase space enclosed in an orbit is minimum if $P_o = \frac{1}{2} r_o$, which is to say that it should be diverging with an angle of $\theta = r_o/2z_o$. In the case of the injector section of Fig. 18, this would require $\theta_f = 3$ mrad rather than $\theta_f = 0$ which was used as a basis for the above table.

This does not conclude the work on the injector, but it does show a way to the solution of radial phase space problems.

APPENDIX

I. ONE DIMENSION TRAVELING WAVE

Defining βc, λ, and F to be the wave velocity, wavelength, and maximum electric field intensity in the accelerator, respectively, and giving other symbols their usual meaning,

$$\frac{dP}{dt} = qF \cos \left(\varphi_o + 2\pi \frac{z - \beta ct}{\lambda} \right) \quad ,$$

$$\frac{dz}{dt} = v \quad ,$$

(A-1)

which can be put into the form

$$\frac{d(P/mc)}{d(\beta ct/\lambda)} = \frac{qF\lambda}{mc^2 \beta} \cos \left[\varphi_o + 2\pi \left(\frac{z}{\lambda} - \frac{\beta ct}{\lambda} \right) \right]$$

$$\frac{d(z/\lambda)}{d(\beta ct/\lambda)} = \frac{v}{\beta c} \quad .$$

This immediately suggests simplifying to dimensionless variables. Old symbols are primed:

$$\frac{z'}{\lambda} = z \qquad\qquad \frac{v'}{c} = v$$

$$\frac{P'}{mc} = P \qquad\qquad \frac{\beta ct'}{\lambda} = t$$

(A-2)

$$\frac{E'}{mc^2} = E \qquad\qquad \frac{qF\lambda}{mc^2} = \alpha \quad .$$

The accelerating field parameter, α, is the electric field intensity in units of particle rest masses/q (0.511 MV for electrons) per wavelength. Now the equations can be written more simply:

$$\frac{dP}{dt} = \frac{\alpha}{\beta} \cos \left[\varphi_o + 2\pi(z - t) \right] \;\; ; \;\; \frac{dz}{dt} = \frac{v}{\beta} \quad .$$

(A-3)

Defining the phase

$$\varphi = \varphi_0 + 2\pi(z - t) \quad , \tag{A-4}$$

which is the amount by which the particle is ahead of the crest of the wave, then

$$\frac{d\varphi}{dz} = 2\pi \left(1 - \frac{\beta}{v}\right) \quad . \tag{A-5}$$

Now Eqs. (A-3), (A-4), and (A-5) can be combined:

$$\frac{dP}{dz} = \frac{\alpha}{v} \cos \varphi$$

$$\frac{dP}{d\varphi} = \frac{\alpha}{2\pi(v - \beta)} \cos \varphi \tag{A-6}$$

$$(v - \beta) \cdot dP = \frac{\alpha}{2\pi} \cos \varphi \, d\varphi \quad .$$

The equations required from special relativity now have particularly simple forms:

$$E^2 = P^2 + 1$$
$$v = \frac{P}{E} = \frac{dE}{dP} \quad . \tag{A-7}$$

Equation (A-6) is easily integrated to give

$$E - \beta P = \frac{\alpha}{2\pi} \sin \varphi + H \quad , \tag{A-8}$$

where H is the constant if integration and can be shown to be the Hamiltonian.[1]

The complete solution needs another equation to show the relationship between z or t, and P, E, or φ. Such an equation is (A-5), but it has not been integrated in closed form.

II. ONE DIMENSION STANDING WAVE

Going back to Eq. (A-3), we can see that the addition of a wave traveling in the opposite direction will give a standing wave

$$\frac{dP}{dt} = \frac{\alpha}{\beta} \cos \left[\varphi_0 + 2\pi(z - t)\right] - \frac{\alpha}{\beta} \cos \left[\varphi_0 + 2\pi(-z - t)\right] \tag{A-9}$$

$$\equiv \frac{2\alpha}{\beta} \sin (2\pi z) \sin (2\pi t - \varphi_0)$$

$$\frac{dz}{dt} = \frac{v}{\beta} \quad .$$

Because of the need to integrate the equations over exactly the same length of accelerator, so that the exit phases be comparable, the equations used were changed to have z as the independent variable

$$\frac{dP}{dz} = \frac{2\alpha}{v} \sin{(2\pi z)} \sin{(2\pi t - \varphi_o)}$$

$$\frac{dt}{dz} = \frac{\beta}{v} \quad .$$

(A-10)

These are the equations for a π-mode standing wave accelerator on the axis of its cylindrical symmetry. Phase is defined the same as in the traveling wave case, Eq. (A-4).

III. CYLINDRICALLY SYMMETRIC STANDING WAVE

Returning to the conventional meaning of symbols for a moment,

$$E_z = FA_z$$

$$A_z = \sum w_n \sin{(kz)} J_0(\gamma r) \sin{(\omega t - \varphi_o)}$$

$$E_r = FA_r$$

$$A_r = -\sum w_n \frac{k}{\gamma} \cos{(kz)} J_1(\gamma r) \sin{(\omega t - \varphi_o)}$$

(A-11)

$$B_\theta = (F/c) A_\theta$$

$$A_\theta = \sum w_n \frac{\omega}{\gamma c} \sin{(kz)} J_1(\gamma r) \cos{(\omega t - \varphi_o)}$$

$$\gamma^2 + k^2 = \omega^2/c^2$$

$$k = 2\pi(2n - 1)/\lambda , \quad n = 1, 2, 3, \ldots$$

Equations (A-11) describe the field at a particle in a cylindrically symmetric accelerator which has planes of symmetry at the center of each wavelength and antisymmetry at the ends of each wavelength.

Neglecting the effect of the transverse velocity on the relativistic mass of the particle, the equation

$$\frac{d\vec{P}}{dt} = q\vec{E} + q\vec{v} \times \vec{B}$$

(A-12)

can be reduced to one in the z direction,

$$\frac{dP}{dt} = qE_z + \dot{r}B_\theta ,$$

(A-13)

and one in the transverse plane,

$$\frac{d\vec{P}_T}{dt} = (qE_r - qvB_\theta)\vec{R}$$

(A-14)

where $\vec{R}$ is the radial unit vector and v is the velocity in the z direction, as before.

Still using conventional notation, E/c^2 is the relativistic particle mass, and

$$\vec{P}_T = \dot{\vec{r}}E/c^2$$

$$\frac{d\vec{P}_T}{dt}c^2 = \ddot{\vec{r}}E + \dot{\vec{r}}\dot{E} \quad .$$

(A-15)

Invoking some fundamental mechanics where R and θ are unit vectors,

$$\dot{\vec{r}} = \dot{r}\vec{R} + r\dot{\theta}\vec{\theta}$$

$$\ddot{\vec{r}} = (\ddot{r} - r\dot{\theta}^2)\,\vec{R} + (2\dot{r}\dot{\theta} + r\ddot{\theta})\,\vec{\theta} \quad .$$

(A-16)

Combining (A-14), (A-15), and (A-16),

$$(\ddot{r} - r\dot{\theta}^2)\,\frac{E}{c^2} + \dot{r}\,\frac{\dot{E}}{c^2} = qE_r - qvB_\theta \; ; \; (2\dot{r}\dot{\theta} + r\ddot{\theta})E + r\dot{\theta}\dot{E} = 0 \quad .$$

(A-17)

In addition to the simplifying definitions (A-2), add

$$\frac{r'}{\lambda} = r \quad .$$

(A-18)

To eliminate the second order derivatives, define

$$s = \frac{\dot{r}'}{c}$$

$$u = \frac{\lambda\dot{\theta}}{c} \quad .$$

(A-19)

Equations (A-7), (A-13), (A-17), and (A-19) reduce, with the definitions in (A-2), (A-11), and (A-18), to:

$$\frac{dE}{dz} = 2\alpha(A_Z + sA_\theta)$$

$$\frac{dt}{dz} = \frac{\beta}{v}$$

$$\frac{ds}{dz} = \frac{ru^2}{v} - \frac{s}{E}\frac{dE}{dz} + \frac{2\alpha}{vE}(A_r - vA_\theta)$$

$$\frac{dr}{dz} = \frac{s}{v}$$

$$\frac{du}{dz} = -\frac{2su}{vr} - \frac{u}{E}\frac{dE}{dz}$$

$$\frac{d\theta}{dz} = \frac{u}{v}$$

$$v = \frac{\sqrt{E^2 - 1}}{E} \quad .$$

(A-20)

In accordance with definitions, the arguments of the auxiliary functions in (A-11) can be somewhat simplified:

$$A_Z = \sum_1^N w_n \sin(Z) \, J_0(R) \sin(T - \varphi_0)$$

$$A_r = -2\pi r \sum_1^N w_n (2n - 1) \cos(Z) \frac{J_1(R)}{R} \sin(T - \varphi_0) \qquad \text{(A-21)}$$

$$A_\theta = 2\pi \, \beta r \sum_1^N w_n \sin(Z) \frac{J_1(R)}{R} \cos(T - \varphi_0) \quad ,$$

where

$$Z = 2\pi(2n - 1)z$$

$$R = 2\pi \sqrt{\beta^2 - (2n - 1)^2} \; r$$

$$T = 2\pi t \quad .$$

By computer, the evaluation of the functions (A-21) and the integration of Eqs. (A-20) are straightforward.

The coefficients w_n can be obtained in theory from the Fourier analysis of a known field. The coefficients actually in use are obtained from T.I. Smith[2] who estimated them by numerically solving Maxwell's equations for the accelerator cavity. The first few coefficients are shown in the table:

n	w_n
1	1.0000
2	-0.0137
3	-0.0106
4	-0.0014
5	+0.0002

---

2. T.I. Smith, private communication.
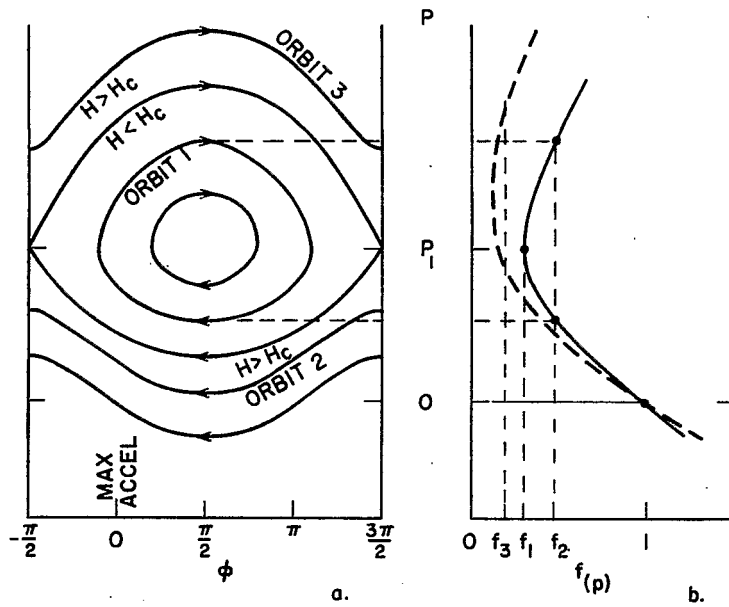
Fig. 1.   Orbits in phase space, traveling wave accelerator.
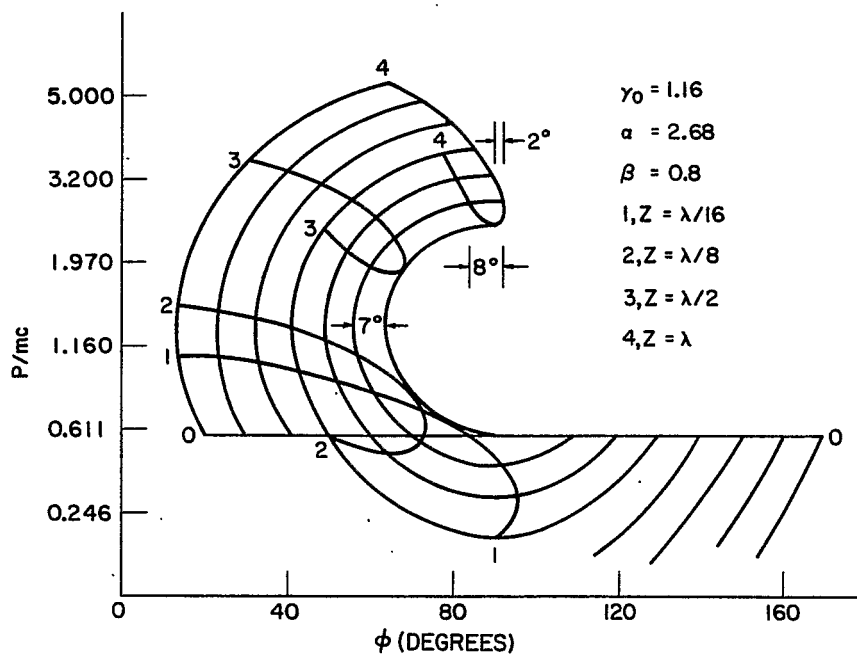
Fig. 2.   Computed orbits in phase space, traveling wave accelerator.
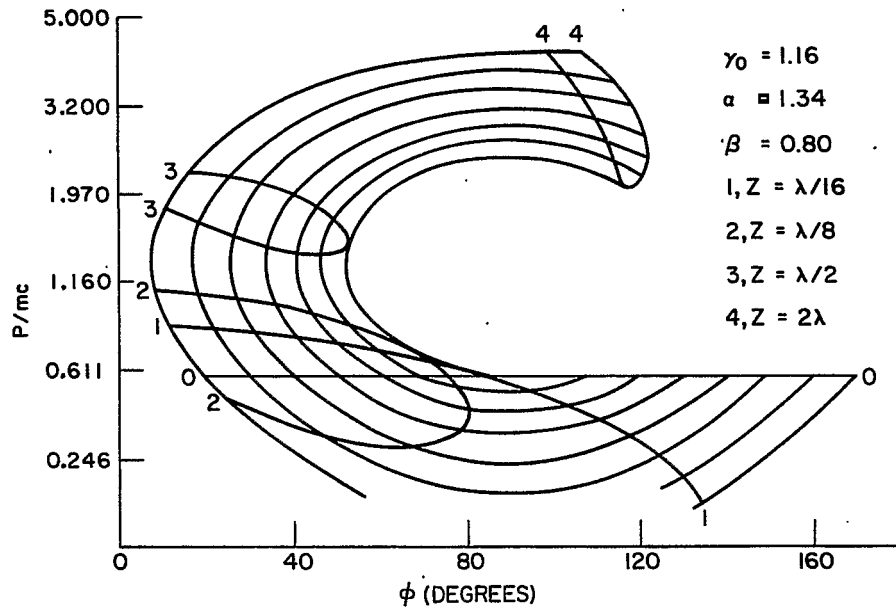
Fig. 3.   Computed orbits in phase space, traveling wave accelerator.
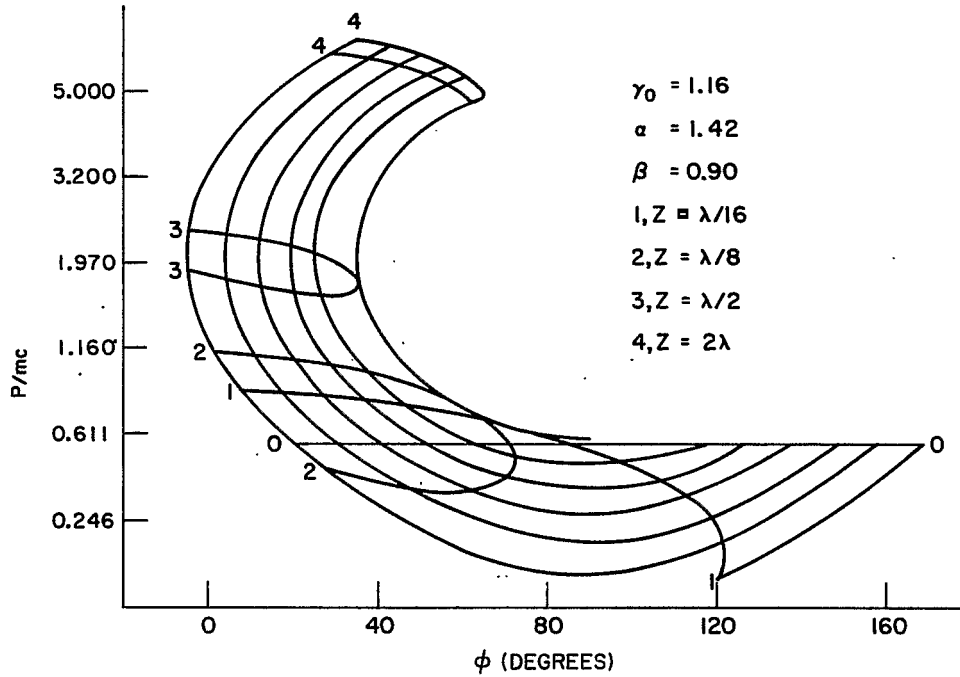
Fig. 4.   Computed orbits in phase space, traveling wave accelerator.
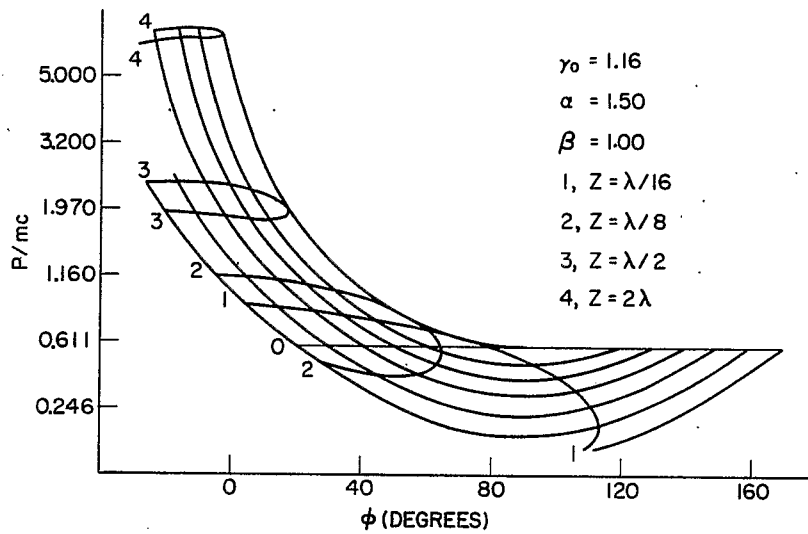
Fig. 5.   Computed orbits in phase space, traveling wave accelerator.
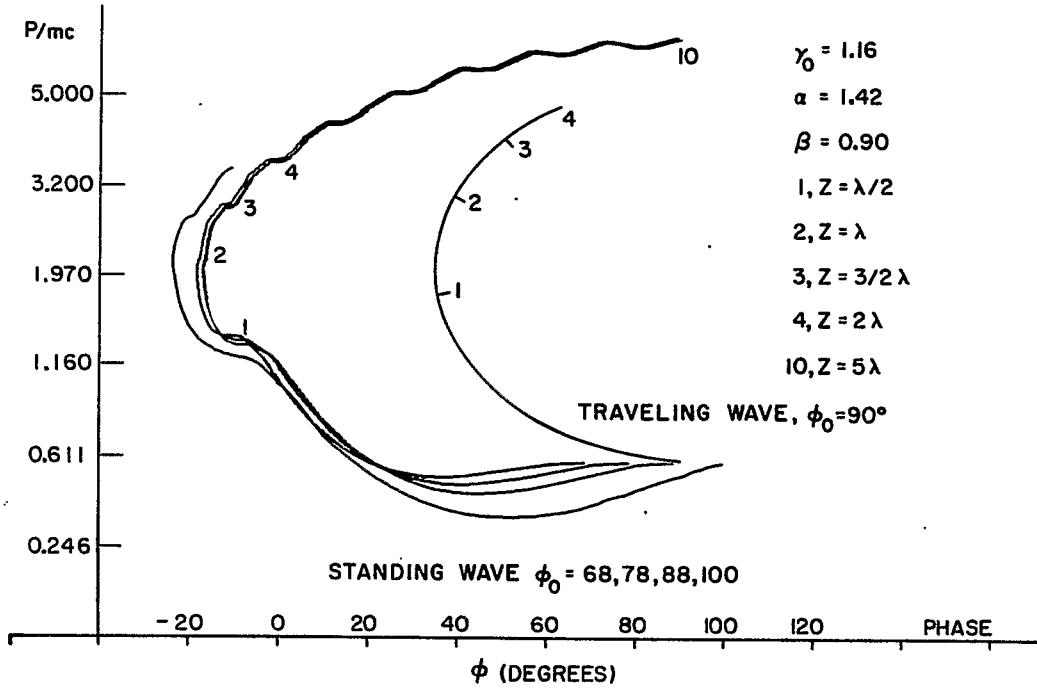
Fig. 6.   Computed orbits in P - φ space, standing wave accelerator.
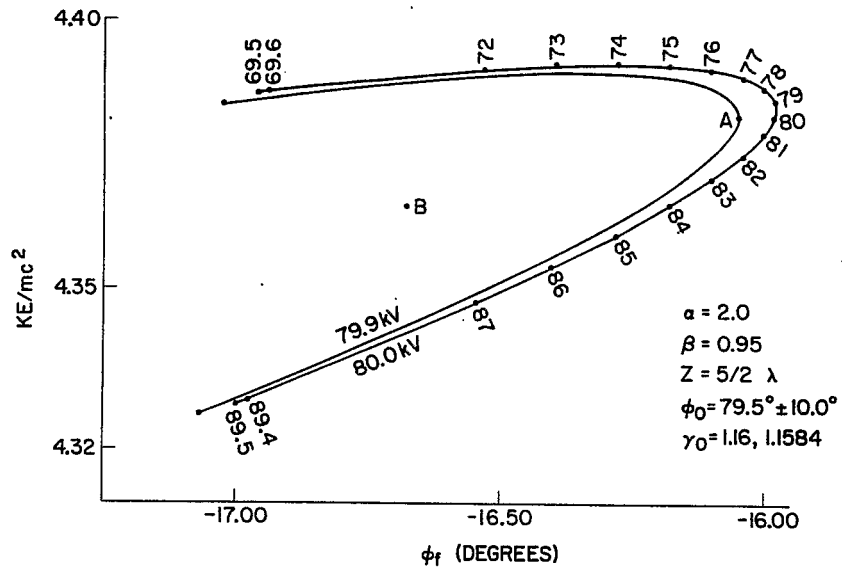
Fig. 7.   The bunch of electrons at exit of 2.5 λ standing wave accelerator section.
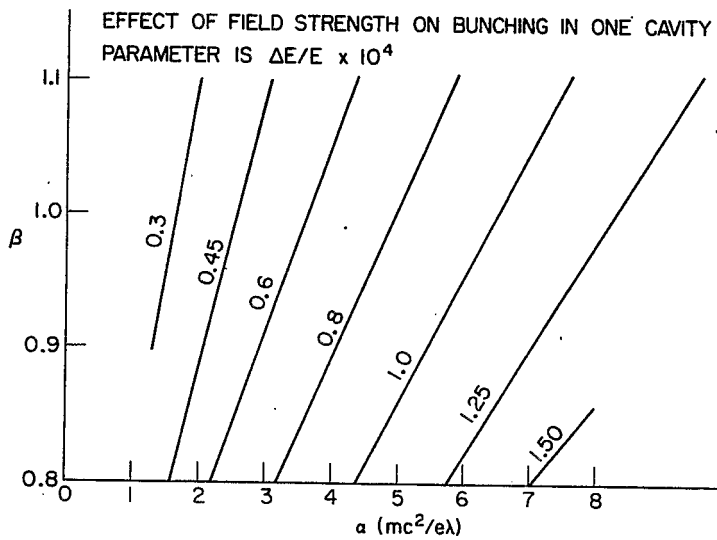
Fig. 8.   Effect of α and β on bunching.
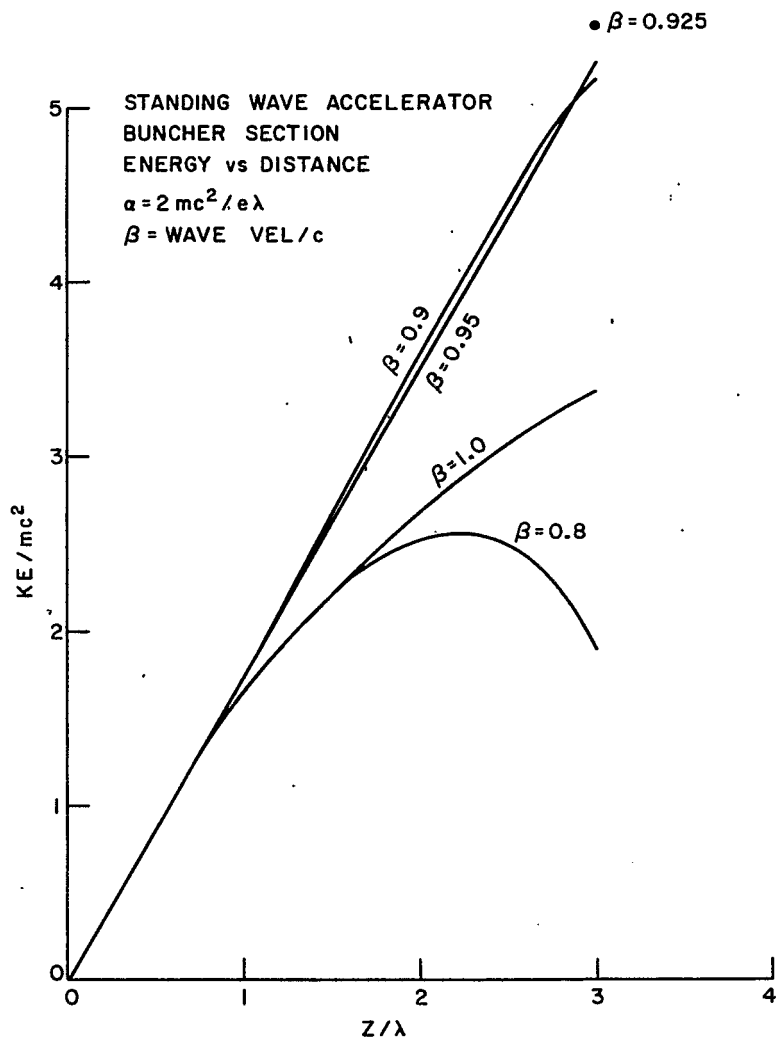
Fig. 9. KE vs Z in buncher section, standing wave.

Fig. 10. Bunch forming in standing wave accelerator.

STANDING WAVE ACCELERATOR
CURRENT PHASE vs INITIAL PHASE

$\alpha = 2mc^2/e\lambda$

$\gamma_0 = 1.16$

$n = 4$

$\beta = 0.95$

PHASE

260°

0

-100°

-100°   0°   80°   160°   260°

INITIAL PHASE

Z = 0
Z = λ/16
Z = λ/18
Z = λ/4
Z = λ/2
Z = λ
Z = 2.5λ
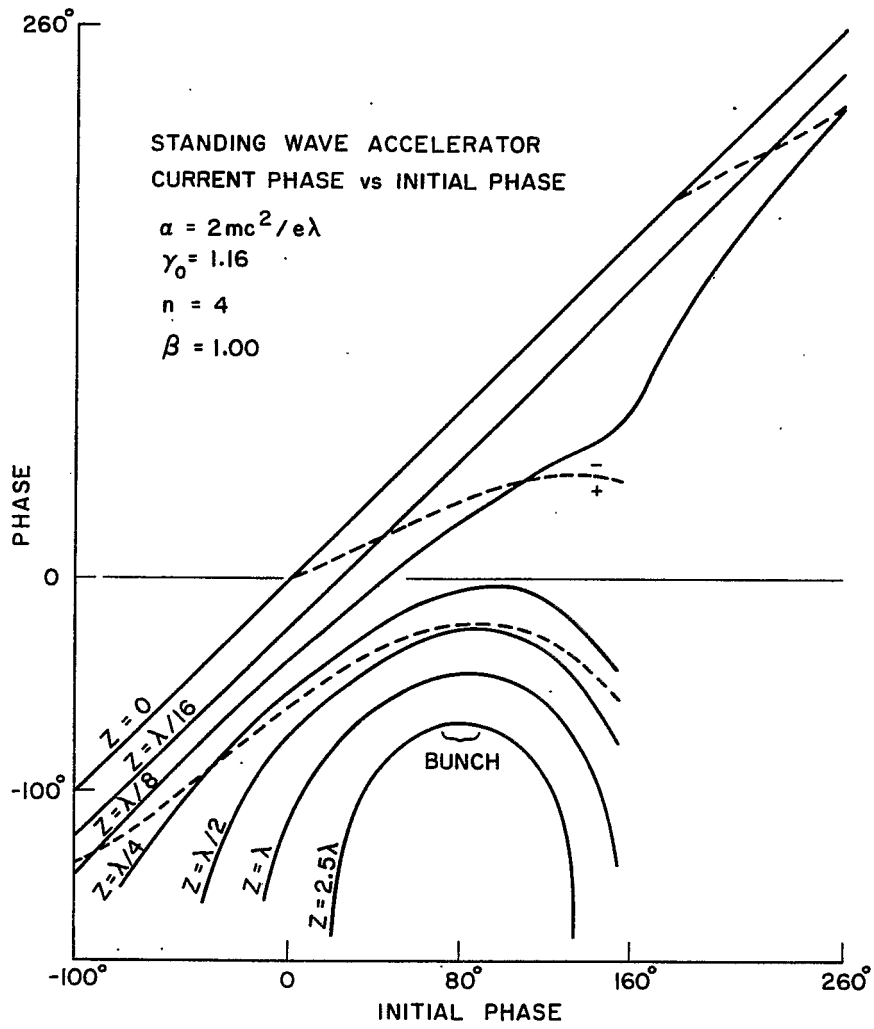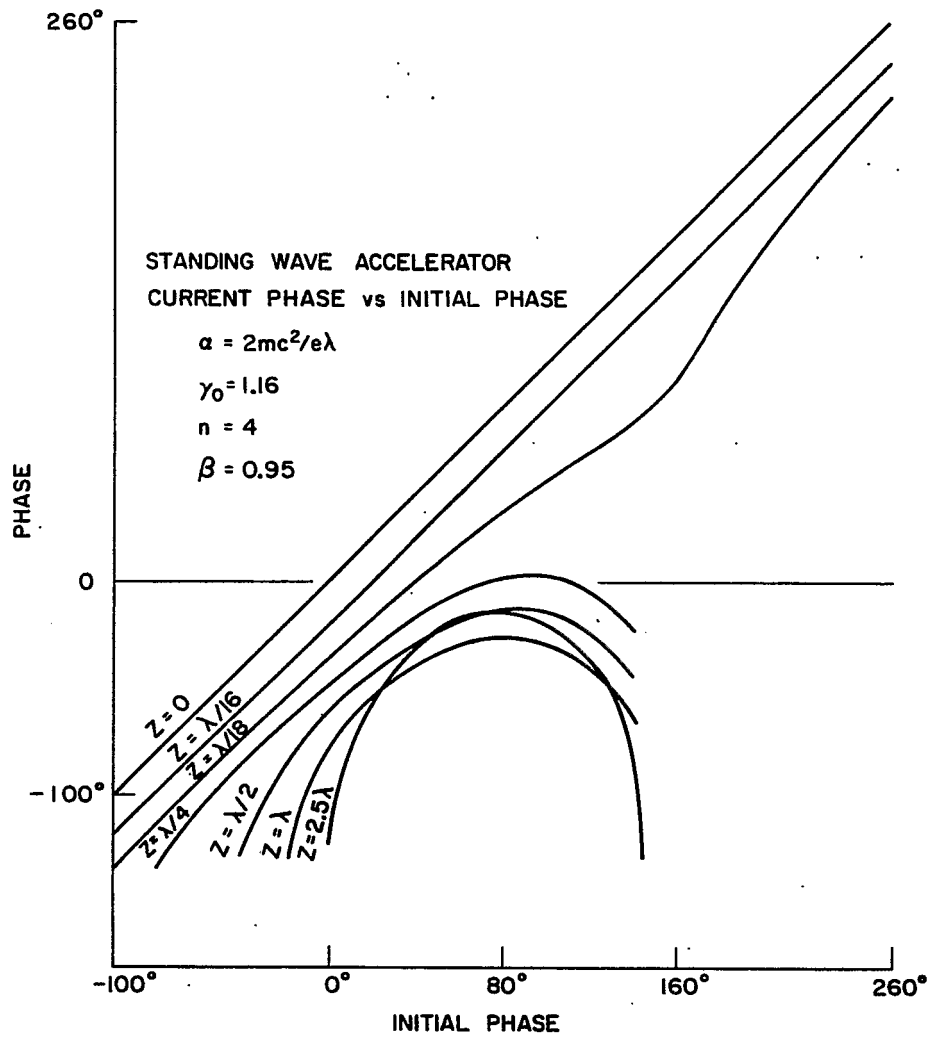
Fig. 11. Bunch forming in standing wave accelerator.
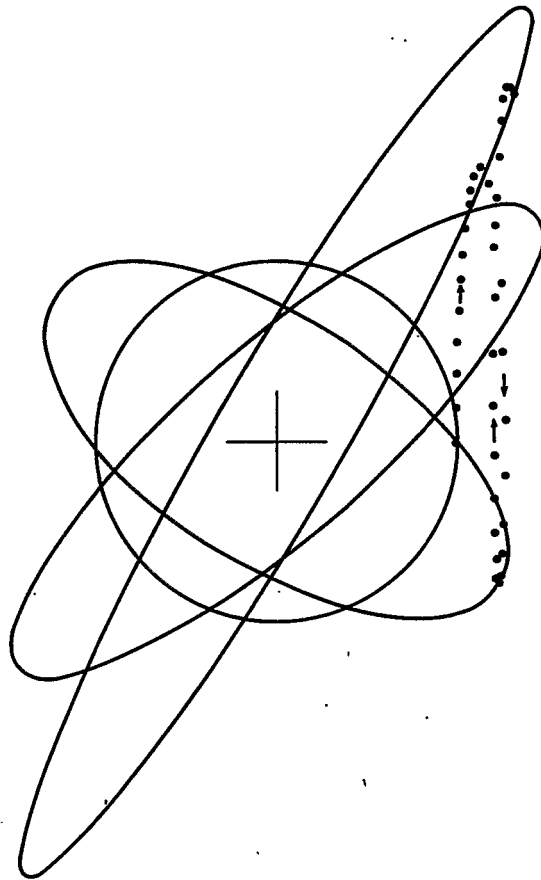
Fig. 12. Orbits and sets in radial phase space.
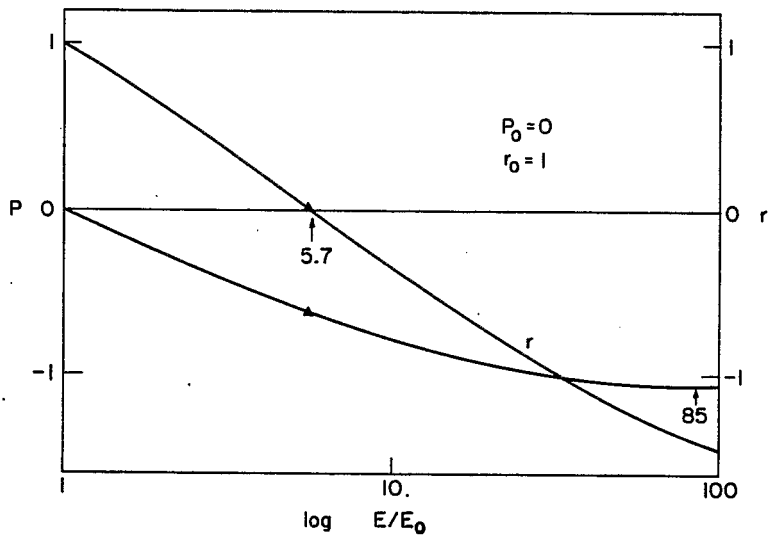
Fig. 13. Radial motion of high energy particles in standard wave accelerator, $r_o = 0$.
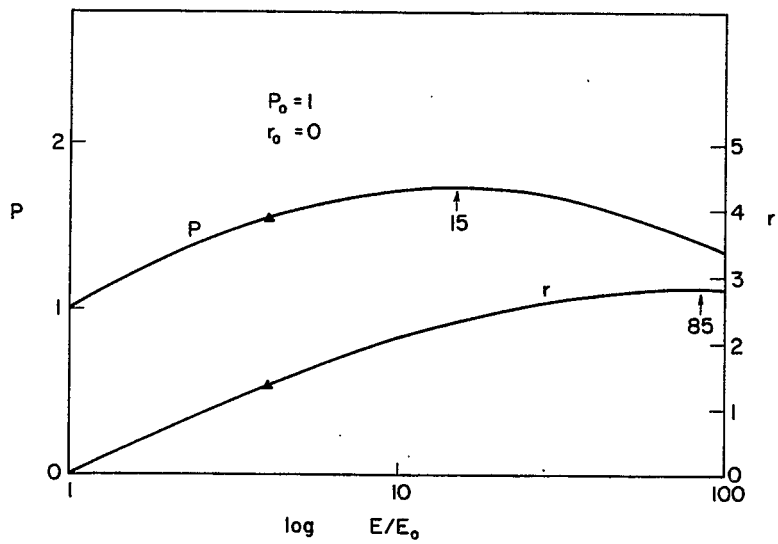
Fig. 14. Radial motion of high energy particles in standard wave accelerator, $P_o = 0$.
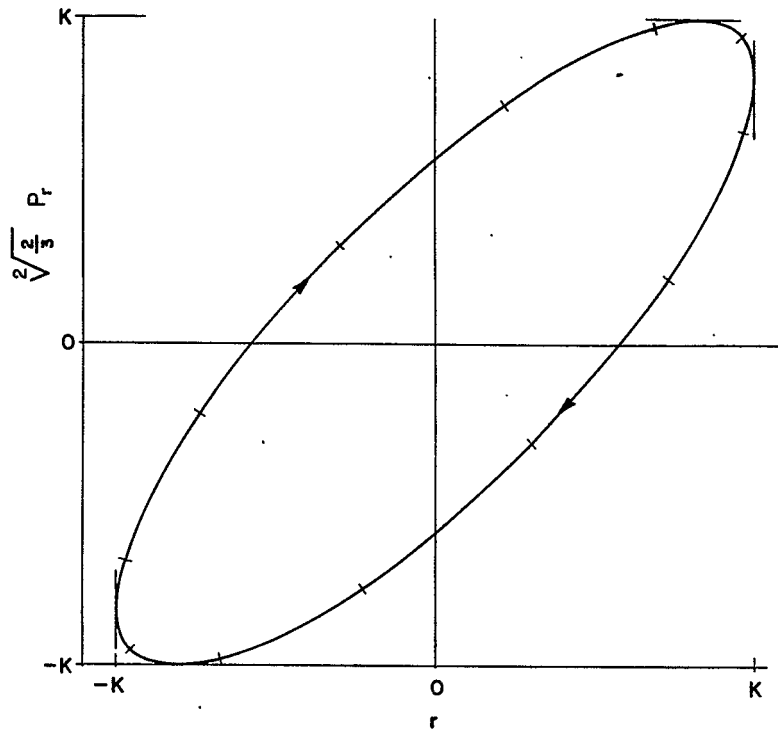
Fig. 15. Radial phase space trajectory in standing wave linac.
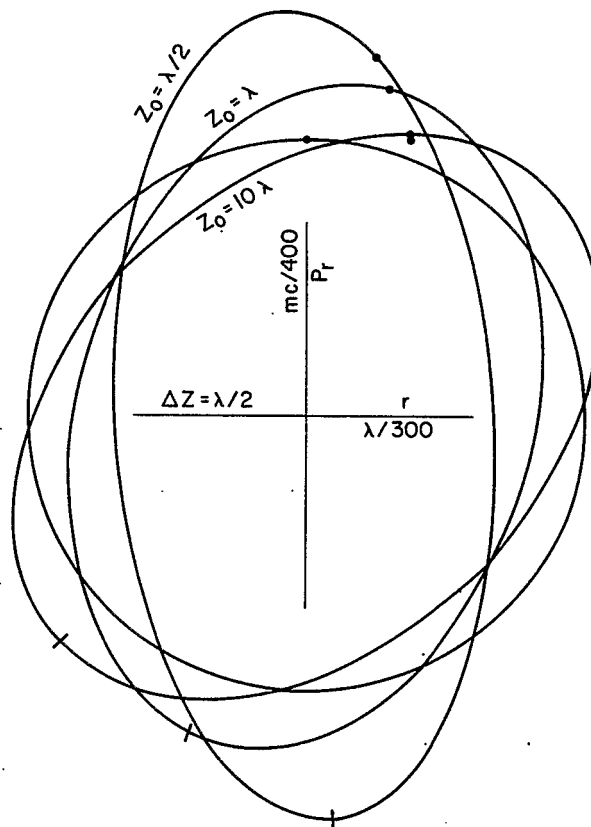
Fig. 16. Sets of relativistic particles in radial phase space, $E \sim M_o C^2$
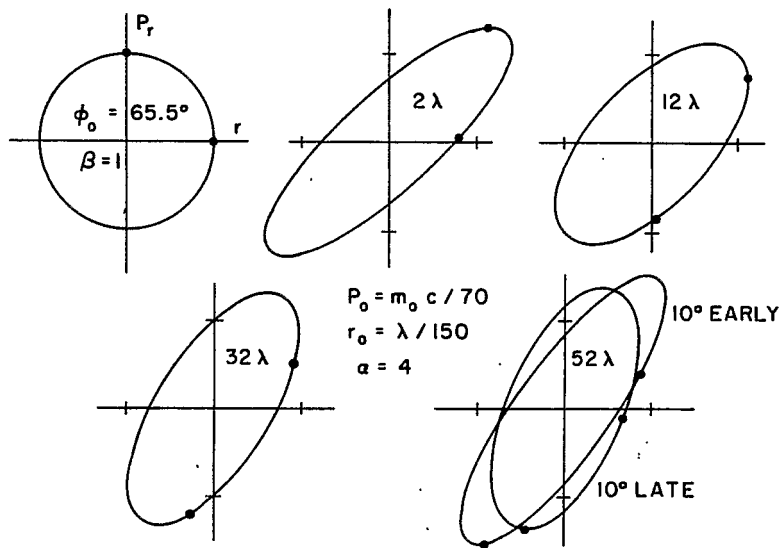
Fig. 17. Set of particles in radial phase space.
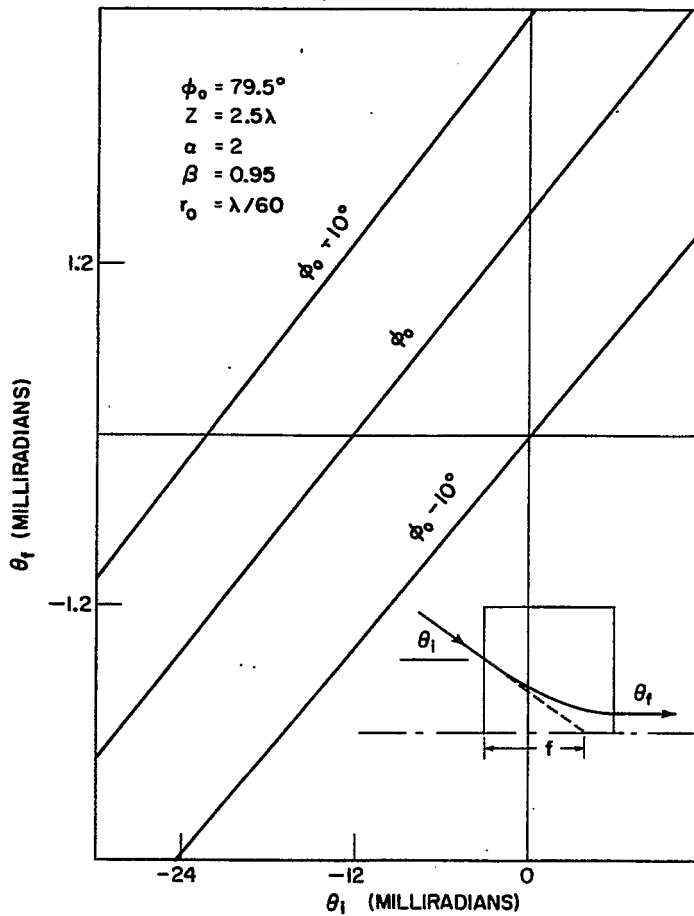
Fig. 18. Lens property of injector section.